MONITORING OF ATMOSPHERIC TRACE GASES OVER CHINA USING GOME AND SCIAMACHY DATA

B. Mijling[(1)], R.J. van der A[(1)], I. De Smedt[(2)], M. Buchwitz[(3)], M. Van Roozendael[(2)], O. Schneising[(3)], I. Khlystova[(3)], H. Bovensmann[(3)], J. P. Burrows[(3)], H. Kelder[(1)]

[(1)] Royal Netherlands Meteorological Institute, P.O. box 201, 3730 AE, De Bilt, The Netherlands; email: mijling@knmi.nl
[(2)] Belgian Institute for Space Aeronomy, Ringlaan-3-Avenue Circulaire, B-1180 Brussels, Belgium; email: Isabelle.Desmedt@bira-iasb.be
[(3)] University of Bremen, Institute of Environmental Physics / Remote Sensing, Otto Hahn Allee 1, 28334 Bremen, Germany; email: Michael.Buchwitz@iup.physik.uni-bremen.de

ABSTRACT

To monitor the air quality over East Asia, we use the measurements of two nadir sounding satellite instruments: GOME on ERS-2 (launched in April 1995) and SCIAMACHY on ENVISAT (launched in June 2001). From the measured spectra, concentrations of important trace gases can be retrieved.

In the first section, the observed NO_2 columns for 2003 are used in a top-down estimate of the anthropogenic NO_x emissions for that year. The emissions in the chemical transport model are adjusted in such a way that the calculated concentrations correspond best with the satellite observations. The new emission estimates show important differences when compared with the EDGAR 3.2 database.

In the second section, the data series of GOME and SCIAMACHY are combined to do retrievals of formaldehyde (CH_2O) from 1996 to 2006. CH_2O is one of the most abundant hydrocarbons and plays a central role in tropospheric chemistry. Its short lifetime combined with the relatively constant methane concentrations in the troposphere, make CH_2O a crucial indicator of biomass burning, isoprene oxidation and other non-methane volatile organic compound oxidation over China. CH_2O columns over Asia seem to increase over the years, but validation by ground measurements is strongly needed.

In the last section, the near-infrared and short-wave-infrared measurements of SCIAMACHY are used to retrieve carbon monoxide (CO), methane (CH_4), and carbon dioxide (CO_2), which are important atmospheric constituents affecting air quality and climate. The CO columns over China correlate well with anthropogenic activity; the high CO columns in South-China at the start of 2004 can be attributed mainly to fires. On average, CH_4 concentrations are highest south of Wuhan and around Chengdu and Chongqing; emissions peak in summer due to rice paddies. A seasonal cycle in CO_2 is found which results from the regular release and uptake of CO_2 by decaying and growing vegetation: maximum CO_2 occurs around April-June, minimum around July-September.

1. TOP-DOWN ESTIMATE OF ANTHROPOGENIC NO_X EMISSIONS

Trend studies [1,15] based on satellite retrievals have shown a significant growth in tropospheric NO_2 columns in China over the last decade, which were attributed to the growth in anthropogenic NO_x emissions. However, quantifying the relation between the local observed NO_2 tropospheric column and the actual NO_x emission is complicated because of non-linear NO_x chemistry and transport of NO_x between grid cells.

In this section a procedure to estimate the anthropogenic NO_x emissions for 2003 in China is presented, based on the observed tropospheric NO_2 columns for that year. Here we only estimated the anthropogenic NO_x emissions from fossil fuel combustion and industry. All other NO_x emissions are referred to as natural emissions and are not estimated.

The measured tropospheric NO_2 columns are retrieved from SCIAMACHY observations [1]. The simulations to determine the modeled tropospheric column as function of the emissions are performed with the chemical-transport model TM5 [9], whereby anthropogenic emissions from the EDGAR 3.2 database [13] are used.

1.1. Relation Between Emissions and Observed Tropospheric Column

To describe the relation between the yearly averaged anthropogenic NO_2 column Ω_{ant} and the yearly anthropogenic NO_x emission E_{ant}, we introduce the parameter α, defined by $\Omega_{ant} = \alpha E_{ant}$. This relation can be assumed linear because of mass conservation [10]. The parameter α is assumed constant for each grid cell, but a wide variation in α along grid cells is found.

Proc. Dragon 1 Programme Final Results 2004–2007, Beijing, P.R. China 21– 25 April 2008 (ESA SP-655, April 2008)

Since the typical size of a grid cell at 1ºx1º resolution over China is ~100 km, transport of NO_x to neighbouring grid cells is –despite its short lifetime– an important factor. NO_x from a source in a particular grid cell is spread out over its neighbouring grid cells, affecting the relation between the local emission and local column. The impact of NO_x transport on the local α is most pronounced in regions with high gradients in tropospheric NO_2. Examples for a few grid cells are shown in Fig. 1.1. The figure shows the anthropogenic NO_x emissions E_{ant} and corresponding anthropogenic NO_2 column Ω_{ant} for the simulations and a linear fit to the data points for each grid cell. Note the wide range in values of α that is found.

The figure shows a high response for areas with high anthropogenic emission levels. This is explained by the fact that only anthropogenic NO_x emissions are increased. At locations with only natural emissions the response will always be zero, if transport effects would be neglected. Only grid cells that are dominated by anthropogenic emissions are included in this study. These grid cells are identified by determining the month of maximum NO_2 concentration, as explained in [1]. Grid cells with a maximum NO_2 in the winter are dominated by anthropogenic emissions, so only grid cells that have a maximum in NO_2 column in December, January or February are included.

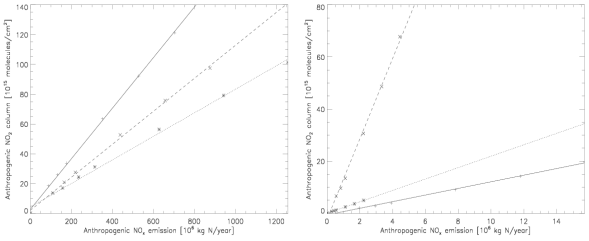

*Figure 1.1. The anthropogenic NO_2 column plotted against anthropogenic NO_x emissions for a selection of 6 grid cells. The left panel shows the relation for Beijing (+), Shanghai (*) and Taipei (X). The linear fit for these three cities is represented by the solid, dotted and dashed line, respectively. The right panel shows this relation for 3 grid cells in rural areas, (longitude, latitude) = (110.5, 32.5), (108.5, 26.5) and (113.5, 32.5), represented by the + symbol, * symbol, and X symbol, respectively.*

1.2. Top-down Estimates

Using the parameter α from the previous section and the yearly averaged SCIAMACHY NO_2 column observations for 2003, the anthropogenic NO_x emission from the top-down estimate E_{td} is determined for every 1ºx1º grid cell. First, the natural column Ω_{nat} is subtracted from the tropospheric NO_2 column Ω_{obs}, thus obtaining an estimate of the anthropogenic NO_2 column measured by satellite. This means E_{td} can be written as:

$$E_{td} = \frac{\Omega_{obs} - \Omega_{nat}}{\alpha} \qquad (1)$$

All other anthropogenic emissions, such as hydrocarbon emissions and CO emissions, have been scaled according to the NO_x emissions in two steps. First, the trend in tropospheric NO_2 is converted to a trend in NO_x emissions using the local linear coefficient α. Thereafter, the change in emission is multiplied by the local ratio of this specific emission and the local NO_x emission.

Performing a model run with the new emissions, still large differences are found between the observed and simulated tropospheric NO_2 column. For most of Eastern China simulated tropospheric NO_2 columns are smaller than the observed columns. However, for some grid cells the TM5 result exceeds the observed tropospheric NO_2 column, most significantly in Korea. The main process causing these differences is the non-uniform rescaling that has been applied to the anthropogenic NO_x emissions (with respect to EDGAR 3.2 anthropogenic NO_x emissions). As a result the amount of modeled NO_x transport between grid cells changes, which will affects the calculated parameter α.

To improve the anthropogenic NO_x emission estimates, an iterative procedure has been used. From the latest simulation a new α is determined as the ratio of the simulated anthropogenic NO_2 column Ω_{ant} and the top-down emissions E_{td}. Again the anthropogenic NO_2 column is found by subtracting the natural NO_2 column from the simulated tropospheric NO_2 column. Then, the new α is used to re-estimate the anthropogenic NO_x emissions based on the observed tropospheric NO_2 columns by SCIAMACHY, according to Eq. 1. Subsequently, the newest anthropogenic NO_x emissions can be checked again by using them in a simulation. Although significant differences exist between observed and simulated tropospheric NO_2 columns persist, differences have generally decreased.

This iterative process is repeated until the difference between the simulated and observed tropospheric NO_2 columns is less than 5%. In this case the iteration has been repeated 4 times. The final results of this procedure are shown in Fig. 1.2.

Fig. 1.2 shows increased anthropogenic NO_x emissions around Beijing and Hong Kong and in the city of Urumqi, in the northwest of China. Also, higher anthropogenic NO_x emissions around the Yellow River can be seen. On the contrary, anthropogenic NO_x emissions around Chengdu and Chongqing have been decreased. Ship track emissions east of China have disappeared in the new emission estimate. The

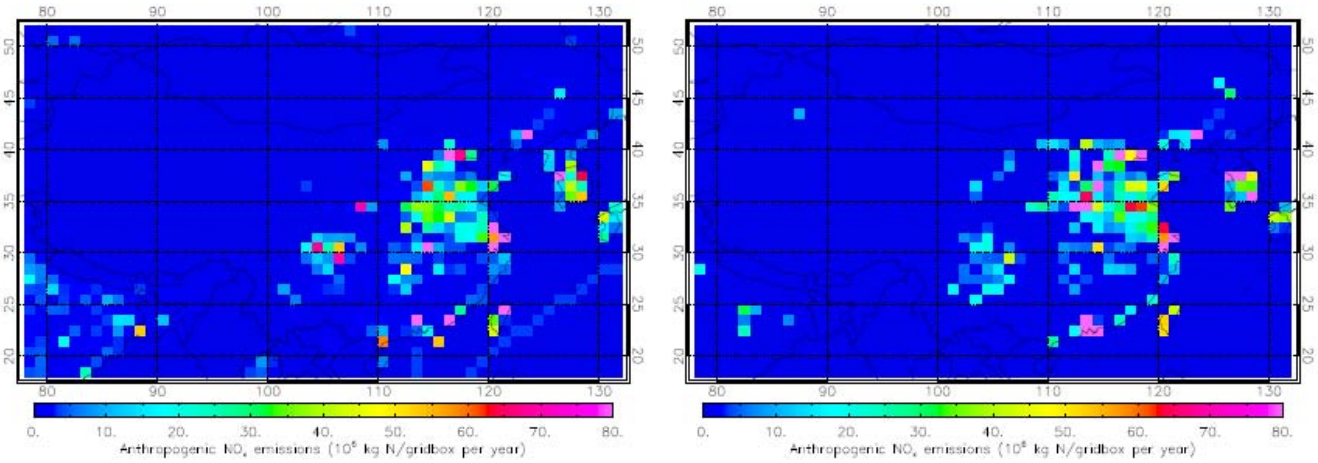

Figure 1.2 The anthropogenic NO_x emissions according to the EDGAR 3.2 database (left panel) and the final emission database from the top-down inventory for 2003 described in this chapter (right panel)

estimated total of anthropogenic NO_x emissions in China in 2003 is 4.33 Tg N, a 31% increase with respect to the anthropogenic NO_x emissions from EDGAR 3.2.

2. RETRIEVAL OF TROPOSPHERIC FORMALDEHYDE (CH_2O)

Formaldehyde (CH_2O) is one of the most abundant hydrocarbons and plays a central role in tropospheric chemistry. It is a short-lived species and an important indicator of non-methane volatile organic compound (NMVOC) emissions and photochemical activity. It is a primary emission product from biomass burning and from fossil fuel combustion, but its principal source in the atmosphere is the photochemical oxidation of methane and non-methane hydrocarbons (NMVOCs). The methane oxidation represents the main CH_2O source accounting for more than half of the globally produced CH_2O, the remainder being produced by NMVOC oxidation. The relatively constant methane concentrations in the troposphere combined with the short lifetime of CH_2O make CH_2O a crucial indicator of biomass burning, isoprene oxidation and other NMVOCs oxidation over the continents. Satellite measurements of CH_2O can be used to constrain VOCs emissions used in current state-of-the-art chemical transport models. In order to perform reliable inverse modeling of emissions, consistent and properly characterized measurements covering several years are required.

In the present work, two satellite instruments have been used: GOME on ERS-2 (launched on the 31st of April 1995) and SCIAMACHY on ENVISAT (launched on the 1st of June 2001). Combining observational data sets from these two UV-visible nadir sounders, tropospheric formaldehyde columns have been retrieved over the period from 1996 until 2006 (Figure 1).

The spectral fit of CH_2O slant column densities (SCDs) is performed using WinDOAS, a multi-purpose DOAS

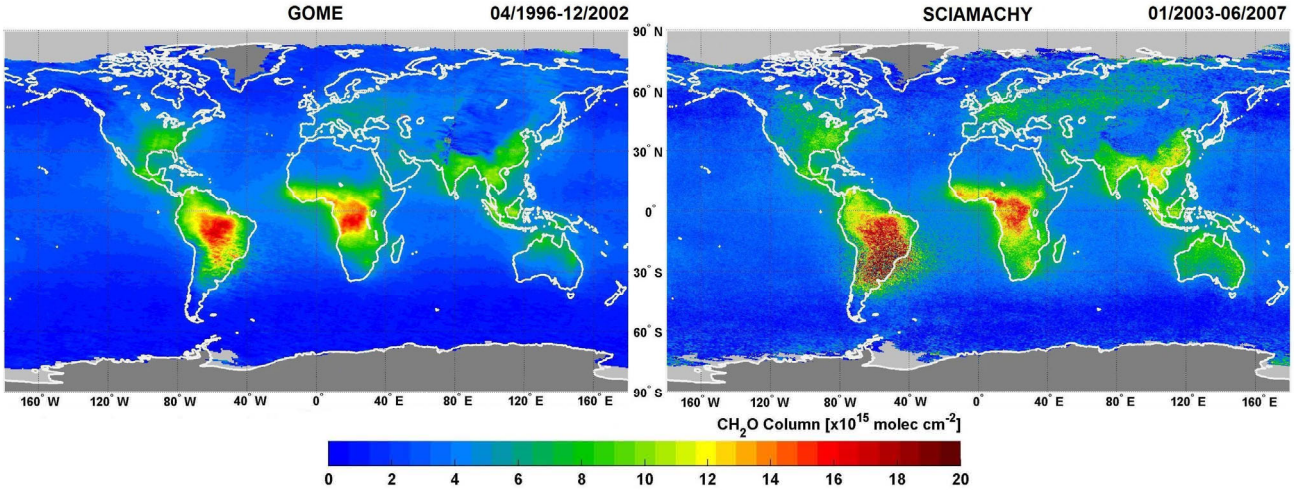

Figure 2.1. CH2O vertical columns retrieved from GOME (1996-2002) and SCIAMACHY (2003-2007)

analysis software developed over the nineties at BIRA-IASB [16]. CH_2O SCDs are retrieved in the 328.5-346 nm spectral range both for GOME and SCIAMACHY spectra. This fitting window has been carefully chosen to produce consistent CH_2O dataset between GOME and SCIAMACHY observations and to minimize artifacts in the background values [De Smedt et al., in preparation].

The second step in the retrieval of tropospheric CH_2O total columns is the calculation of the air mass factor that is needed to convert DOAS slant columns into corresponding vertical columns. Because of UV scattering by air molecules, clouds and aerosols, the AMF is sensitive to the vertical distribution of the absorbing molecule and to the surface albedo. As a consequence, air mass factors cannot be derived from straightforward geometric considerations, but instead require full multiple scattering calculations. However, if the trace gas under investigation has a small absorption optical thickness, it is possible to separate the scattering properties of the atmosphere from the vertical distribution of the absorber [14].

In this work, weighting functions have been evaluated from radiative transfer calculations performed with a pseudo-spherical version of the DISORT code [20]. Best-guess profiles of CH_2O are provided by the IMAGES model on a monthly basis [12]. A cloud correction is based on the independant pixel approximation [11]. Cloud fraction and cloud top height informations are obtained using the FRESCO cloud product [8]. Fig. 2.1 shows the CH_2O vertical columns retreived from GOME between April 1996 and December 2002 and from SCIAMACHY between January 2003 and June 2007.

Fig.2.2 shows the yearly mean of CH_2O from 1996 to 2006 in Asia. From 2003 onward, the better resolution of SCIAMACHY allows identifying localized regions of emissions but the data are also noisier because of the resulting shorter integration time. There seems to be an increase in the CH_2O columns over the years in several regions of Asia but uncertainties are too large to draw conclusions. Therefore, there is a strong need for ground-based measurements to validate the satellite data in this region of the world.

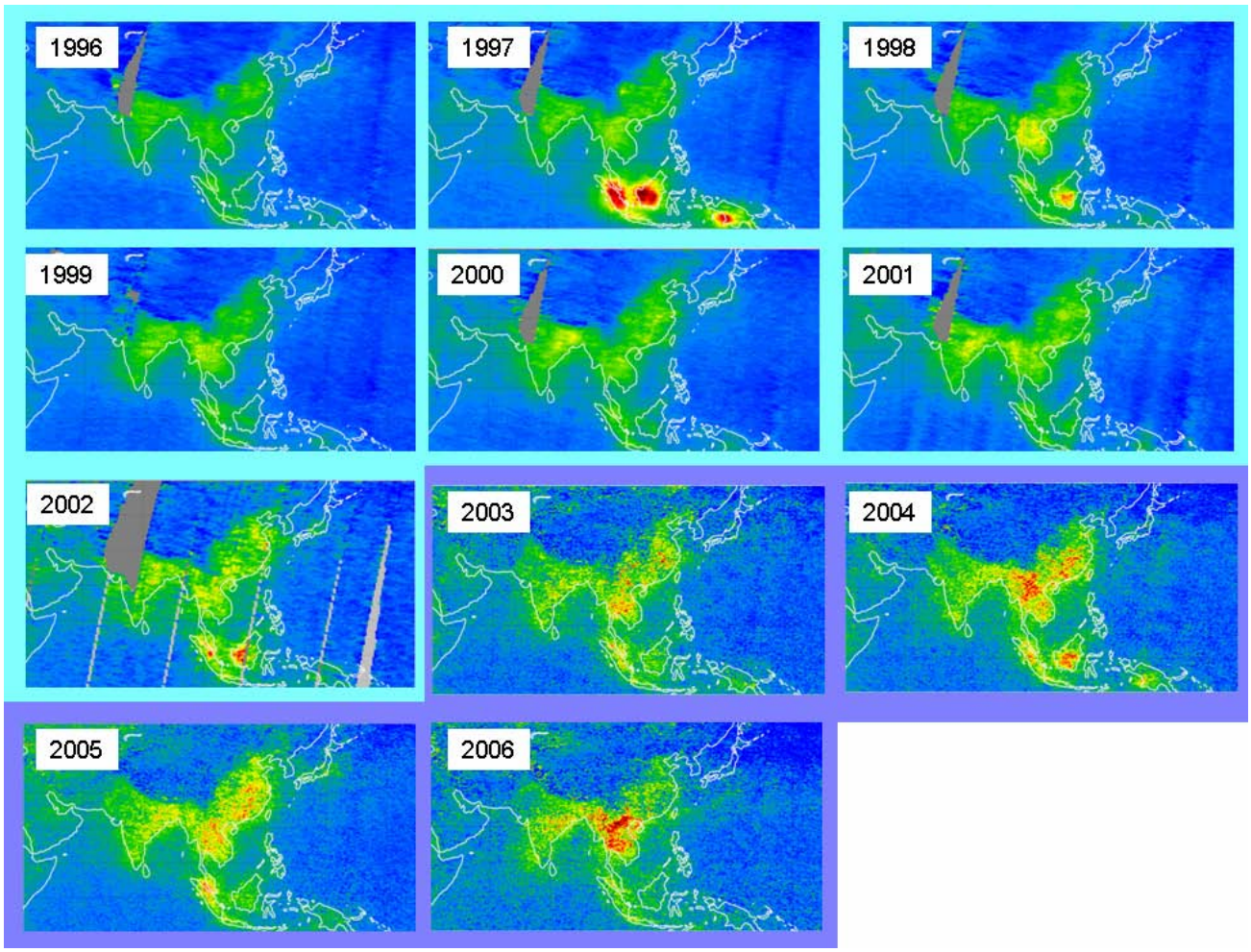

Figure 2.2. Climatology of CH2O vertical columns retrieved from GOME (1996-2002) and SCIAMACHY (2003-2007) in Asia.

3. CARBON MONOXIDE, METHANE AND CARBON DIOXIDE AS RETRIEVED FROM SCIAMACHY NEAR-INFRARED NADIR SPECTRA

3.1. Introduction

The three carbon atom containing gases carbon monoxide (CO), methane (CH_4), and carbon dioxide (CO_2) are important atmospheric constituents affecting air quality and climate. The near-infrared (NIR) / short-wave-infrared (SWIR) nadir measurements of reflected and backscattered solar radiation as recorded by SCIAMACHY onboard ENVISAT enable the retrieval of vertical columns or column-averaged mixing ratios of these gases with high sensitivity down to the Earth's surface where their source signal is largest.

Recently, three years (2003-2005) of SCIAMACHY data have been (re)processed using the latest versions of the scientific retrieval algorithm WFM-DOAS (CO version 0.6, methane and CO_2 version 1.0) which have been significantly improved compared to the previous version 0.5 discussed in [3]. Details about the new retrieval algorithms and corresponding global data sets are given in [4] for CO, [5] for CO_2, and [17] for methane. A detailed assessment of the quality of these data sets is the focus of current activities. A first validation of the CO and CH_4 data sets has been performed by [6] using ground-based FTIR measurements focusing on Europe and the years 2003 and 2004. Here we present a short overview about these data sets focusing on China and on the year 2004.

3.2. Carbon Monoxide

Carbon monoxide (CO) vertical columns are retrieved using the WFM-DOAS version 0.6 retrieval algorithm [4] from a small spectral fitting window (2324.4-2335.0 nm) located in SCIAMACHY channel 8 covering several absorption lines of CO. Fig. 3.1 shows the retrieved CO columns over China and surrounding countries during 2004. As can be seen, CO columns are highest in the eastern part of China in the region between Beijing and Wuhan, but also in southern China around Hong Kong and in the area of the two large cities Chengdu and Chongqing. The CO columns over China correlate well with population density which is a good proxy for anthropogenic (e.g., industry, traffic, domestic heating) emissions. South of China, over south-east Asia, where population density is lower, CO is also high, especially in the first few months of 2004, mostly due to CO emissions from fires. It appears that CO emissions from China during 2004 are higher than the CO emissions from India.

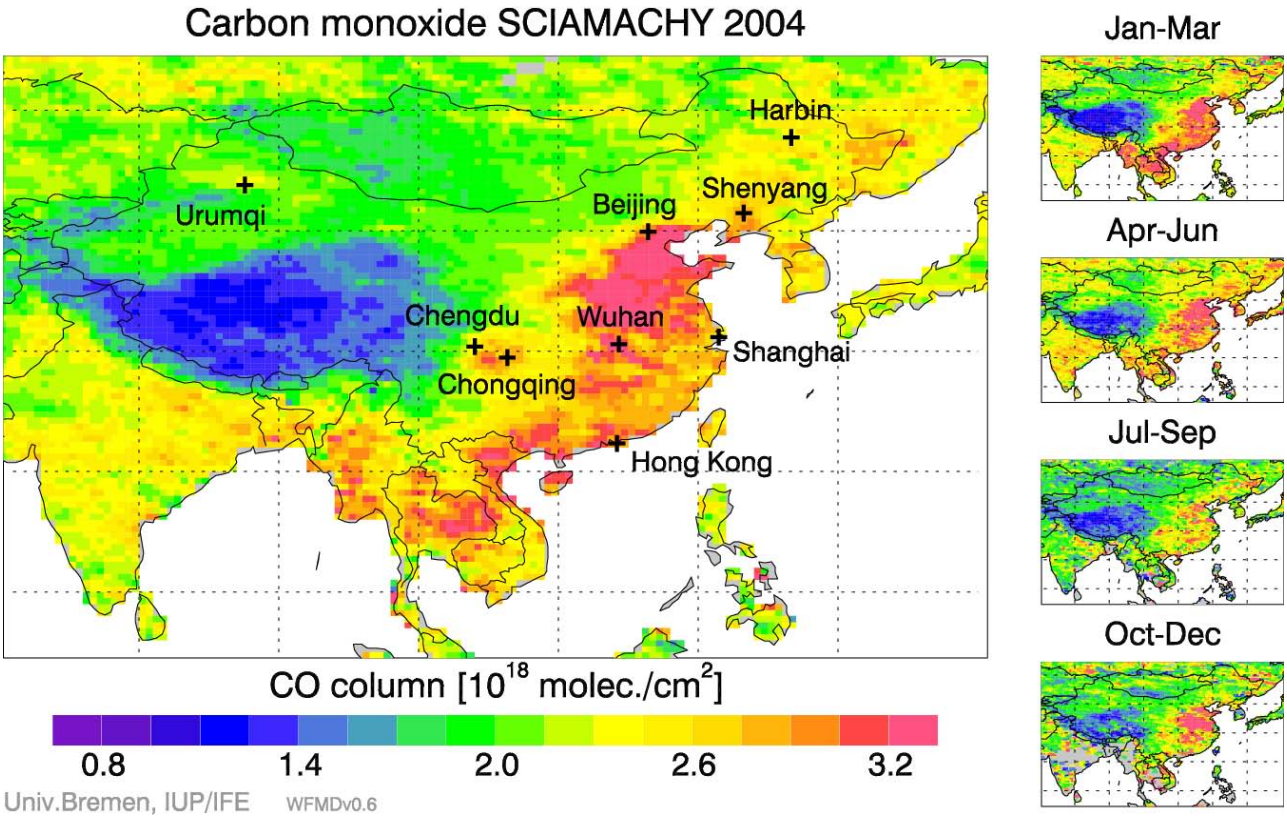

Figure 3.1. Carbon monoxide (CO) vertical columns over China as retrieved from SCIAMACHY. The year 2004 annual composite map is shown on the left hand side and on the right seasonal averages corresponding to January-March 2004 (top) to October-December 2004 (bottom) are depicted.

3.3. Methane

Methane (CH_4) vertical columns are retrieved from a small spectral fitting window located in SCIAMACHY channel 6. Following the method first proposed by [7] CO_2 from channel 6 is used as a proxy for the light path and the CO_2 column is used to estimate the air column needed to compute the column-averaged dry air mole fraction or mixing ratio of methane, denoted XCH_4. The latest version of the retrieval algorithm is WFM-DOAS version 1.0 [17,19]. Fig. 3.2 shows the retrieved XCH_4 over China during 2004. As can be seen, methane concentrations are highest south of Wuhan and around Chengdu and Chongqing. Major methane sources are rice paddies, wetland and ruminants (see, e.g. [2] and references given therein). Methane emissions are highest in summer as can be clearly seen in Fig. 3.2 where it is also shown that methane is not only high over China but also over India (e.g., rice emissions) and Russia (e.g., wetland emissions), especially during July-September but also later in the year.

3.4. Carbon Dioxide

Carbon dioxide (CO2) vertical columns are retrieved from a small spectral fitting window located in SCIAMACHY channel. Oxygen (O_2) from channel 4 is used as a proxy for the light path and the O_2 column is used to estimate the air column needed to compute the column-averaged dry air mole fraction or mixing ratio of carbon dioxide, denoted XCO_2. The latest version of the retrieval algorithm is WFM-DOAS version 1.0 [5,18]. Fig 3.3 shows the retrieved XCO_2 over China during 2004. As can be seen from the seasonal averages, maximum CO_2 occurs around April-June, minimum CO_2 around July-September, especially at higher latitudes. This is due to the CO_2 seasonal cycle which results from the regular release and uptake of CO_2 by decaying and growing vegetation. More details on the CO_2 seasonal cycle as observed by SCIAMACHY are given in [5]. Fig 3.3 shows that there are large data gaps in the seasonal averages. This is due to the strict quality filtering used for the CO_2 retrievals rejecting many measurements for example because of clouds. As a result, the annual composite

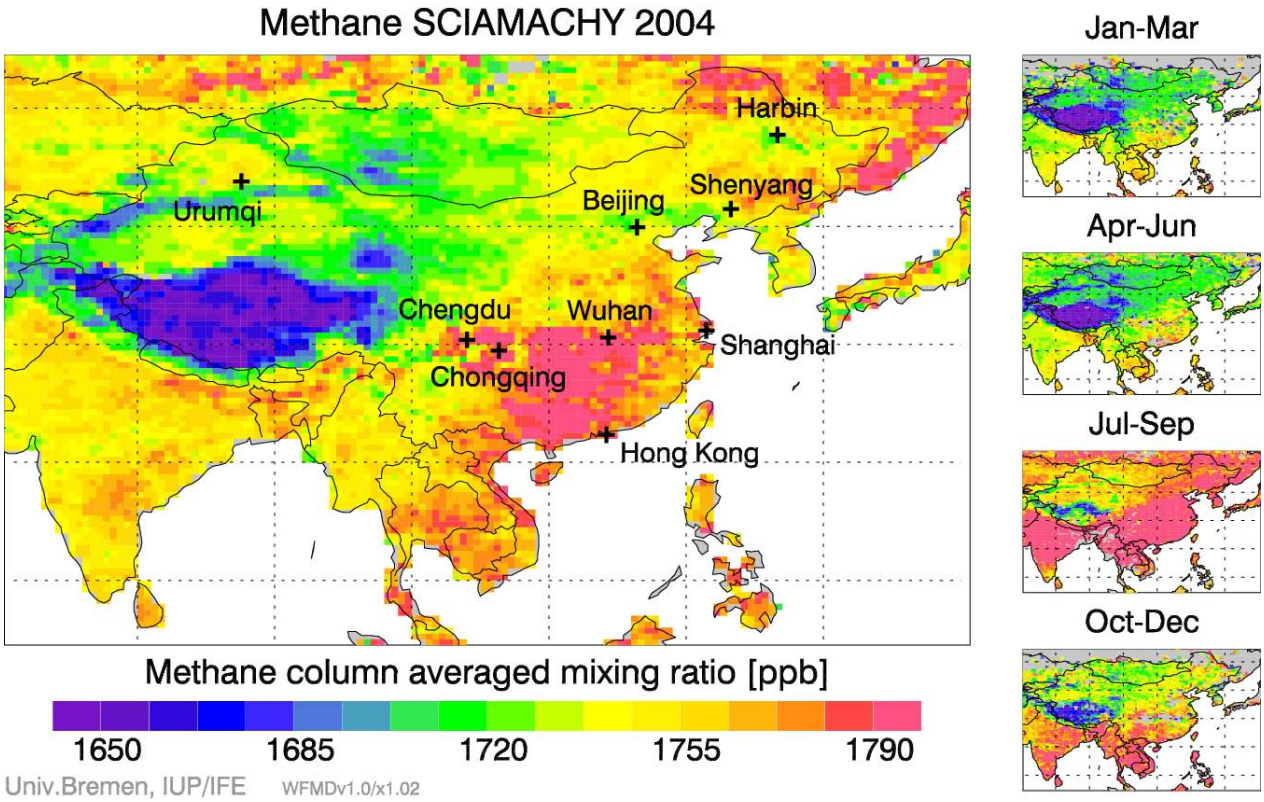

Figure 3.2. As Figure 2.1 but for methane (CH_4).

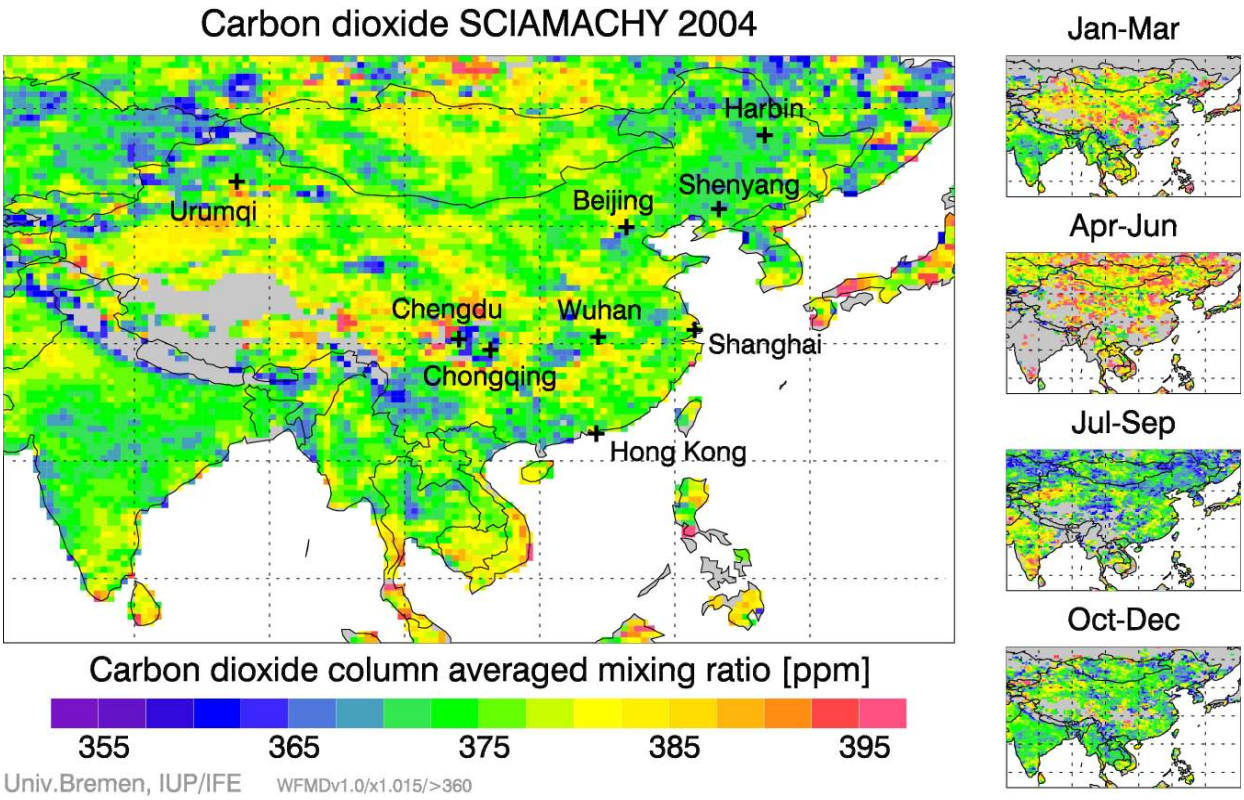

Figure 3.3. As Figure 3.1 but for carbon dioxide (CO_2).

map does not represent the yearly average but reflects the inhomogeneous sampling of the satellite data which must be considered when interpreting the data in terms of CO_2 sources and sinks.

4. CONCLUSIONS

The observed NO_2 columns for 2003 by SCIAMACHY are used in a top-down estimate of the anthropogenic NOx emissions for that year. The emissions in TM5 are adjusted iteratively such that the calculated concentrations correspond best with the satellite observations. The new emission estimates show important differences when compared with the EDGAR 3.2 database: higher around Beijing, Hong Kong, Urumqi. and around the Yellow River; lower around Chengdu and Chongqing. The estimated total of anthropogenic NO_x emissions increases 31% with respect to EDGAR 3.2.

The data series of GOME and SCIAMACHY can be combined to do retrievals of CH_2O from 1996 to 2006. SCIAMACHY data gives better resolution, but also noisier data due to a shorter integration time. CH_2O columns over Asia seem to increase over the years, but there is a strong need for validation by ground measurements.

The near-infrared and short-wave-infrared measurements of SCIAMACHY are used to retrieve CO, CH_4 and CO_2. The CO columns over China correlate well with anthropogenic activity; the high CO columns in South-China at the start of 2004 can be attributed mainly to fires. On average, CH_4 concentrations are highest south of Wuhan and around Chengdu and Chongqing. CH_4 emissions peak in summer due to rice paddies. There is a seasonal cycle in CO_2 which results from the regular release and uptake of CO_2 by decaying and growing vegetation: maximum CO_2 occurs around April-June, minimum CO_2 around July-September, especially at higher latitudes.

5. REFERENCES

1. van der A, R.J., D.H.M.U. Peters, H. Eskes, K.F. Boersma, M. Van Roozendael, I. De Smedt, H.M. Kelder, Detection of the trend and seasonal variation in tropospheric NO2 over China, J. Geophys. Res., 111, doi:10.1029/2005JD006594, 2006.
2. Bergamaschi, P., C. Frankenberg, J. F. Meirink, M. Krol, F. Dentener, T. Wagner, U. Platt, J. O. Kaplan, S. Körner, M. Heimann, E. J. Dlugokencky, A. and Goede, Satellite chartography of atmospheric methane from SCIAMACHY onboard ENVISAT: 2. Evaluation based on inverse model simulations, J. Geophys.

Res. 112, D02304, doi:10.1029/2006JD007268, 2007.

3. Buchwitz, M., R. de Beek, S. Noël, J. P. Burrows, H. Bovensmann, O. Schneising, I. Khlystova, M. Bruns, H. Bremer, P. Bergamaschi, S. Körner, M. Heimann, Atmospheric carbon gases retrieved from SCIAMACHY by WFM-DOAS: version 0.5 CO and CH4 and impact of calibration improvements on CO2 retrieval, Atmos. Chem. Phys., 6, 2727-2751, 2006.
4. Buchwitz, M., I. Khlystova, H. Bovensmann, J. P. Burrows, Three years of global carbon monoxide from SCIAMACHY: Comparison with MOPITT and first results related to the detection of enhanced CO over cities, Atmos. Chem. Phys., 7, 2399-2411, 2007a.
5. Buchwitz, M., O. Schneising, J. P. Burrows, H. Bovensmann, M. Reuter, J. Notholt, First direct observation of the atmospheric CO2 year-to-year increase from space, Atmos. Chem. Phys., 7, 4249-4256, 2007b.
6. Dils, B., De Maziere, M., Blumenstock, T., Hase, F., Kramer, I., Mahieu, E., Demoulin, P., Duchatelet, P., Mellqvist, J., Strandberg, A., Buchwitz, M., Khlystova, I., Schneising, O., Velazco, V., Notholt, J., Sussmann, R., and Stremme, W., Validation of WFM-DOAS v0.6 CO and v1.0 CH4 scientific products using European ground-based FTIR measurements, proceedings of the Third Workshop on the Atmospheric Chemistry Validation of ENVISAT (ACVE-3), 4-7 Dec. 2006, ESA/ESRIN, Frascati, Italy, ESA Publications Division Special Publication SP-642 (CD), 2006.
7. Frankenberg, C., J. F. Meirink, M. van Weele, U. Platt, and T. Wagner, Assessing methane emissions from global spaceborne observations, Science, 308: 1010-1014, 2005.
8. Koelemeijer, R. B. A., P. Stammes, J. W. Hovenier, and J. F. de Haan, Global distributions of effective cloud fraction and cloud top pressure derived from oxygen A band spectra measured by the Global Ozone Monitoring Experiment: comparison to ISCCP data, J. Geophys. Res., 107(D12), 4151, doi: 10.1029/2001JD000840, 2002.
9. Krol, M., S. Houweling, B. Bregman, M. van den Broek, A. Segers, P. van Velthoven, W. Peters, F. Dentener and P. Bergamaschi, The two-way nested global chemistry-transport zoom model TM5: algorithm and applications, Atmos. Chem. Phys., 5, 417-432, 2005.
10. Martin, R.V., D.J. Jacob, K.V. Chance, T.P. Kurosu, P.I. Palmer, and M.J. Evans, Global inventory of Nitrogen Dioxide Emissions Constrained by Space-based Observations of NO2 Columns, J. Geophys. Res., 108(D17), 4537, doi:10.1029/2003/JD003453, 2003.
11. Martin, R.V., K. Chance, D. J. Jacob, T. P. Kurosu, R. J. D. Spurr, E.Bucsela, J. F. Gleason, P. I. Palmer, I. Bey, A. M. Fiore, Q. Li, R. M. Yantosca and R. B. A. Koelemeijer, An improved retrieval of tropospheric nitrogen dioxide from GOME, J. Geophys. Res., 107(D20), 4437, 2001.
12. Müller, J.-F., and T. Stavrakou, Inversion of CO and NOx emissions using the adjoint of the IMAGES model, Atmos. Chem. Phys. 5, 1157-1186, 2005
13. Olivier, J.G.J., A.F. Bouwman, Van Der Hoek, K.W. and J.J.M. Berdowski, Global Air Emission Inventories for Anthropogenic Sources of NOx, NH3 and N2O in 1990, Env. Poll., 102, 135-148, 1998.
14. Palmer, P. I., D. J. Jacob, K. Chance, R. V. Martin, R. J. D. Spurr, T. P. Kurosu, I. Bey, R. Yantosca, A. Fiore, and Q. Li, Air-mass factor formulation for spectroscopic measurements from satellites: application to formaldehyde retrievals from GOME, J. Geophys. Res., 106, 14,539-14,550, 2001.
15. Richter, A., K., J.P. Burrows, H. Nüß, C. Granier, and . Niemeier (2005), Increase in tropospheric nitrogen dioxide over China observed from space, Nature, 437, doi:10.1038/nature04092, 2005.
16. Roozendael, M. van, C. Fayt, J.-C. Lambert, I. Pundt, T. Wagner, A. Richter, and K. Chance, Development of a bromine oxide product from GOME, in Proc. ESAMS'99, WPP-161, p. 543-547, 1999.
17. Schneising, O., M. Buchwitz, H. Bovensmann, and J. P. Burrows, Three years of SCIAMACHY carbon dioxide and methane column-averaged dry air mole fraction measurements, Proceedings ENVISAT Symposium 2007, Montreux, Switzerland, 23-27 April 2007, ESA publications division SP-636 (CD), p. 4, 2007a.
18. Schneising, O., M. Buchwitz, J. P. Burrows, et al., Three years of greenhouse gas column-averaged dry air mole fractions retrieved from satellite - Part 1: Carbon dioxide, manuscript in preparation, 2007b.
19. Schneising, O., M. Buchwitz, J. P. Burrows, et al., Three years of greenhouse gas column-averaged dry air mole fractions retrieved from satellite - Part 2: Methane, manuscript in preparation, 2007c.
20. Stamnes, K., SC Tsay, K Jayaweera, W Wiscombe, Numerically Stable Algorithm For Discrete-Ordinate-Method Radiative Transfer in Multiple Scattering and Emitting